Synergy of SMC and Topoisomerase Creates a Universal Pathway to Simplify Genome Topology

Enzo Orlandini,[1] Davide Marenduzzo,[2] and Davide Michieletto[2]

[1]*Dipartimento di Fisica e Astronomia "Galileo Galilei", sezione INFN, Università degli Studi di Padova, via Marzolo 8, I-35131 Padova, Italy.*

[2]*School of Physics and Astronomy, University of Edinburgh, Peter Guthrie Tait Road, Edinburgh, EH9 3FD, UK*

Topological entanglements severely interfere with important biological processes. For this reason, genomes must be kept unknotted and unlinked during most of a cell cycle. Type 2 Topoisomerase (TopoII) enzymes play an important role in this process but the precise mechanisms yielding systematic disentanglement of DNA *in vivo* are not clear. Here we report computational evidence that Structural Maintenance of Chromosomes (SMC) proteins – such as cohesins and condensins – can cooperate with TopoII to establish a synergistic mechanism to resolve topological entanglements: SMC-driven loop extrusion (or diffusion) induces the spatial localisation of entanglements in turn increasing the topological pressure within knotted or linked regions. As a consequence, knots, links and ensuing entanglements may be readily simplified by Topoisomerase enzymes even in crowded and confined conditions. The mechanism we uncover is universal in that it does not qualitatively depend on the specific substrate, whether DNA or chromatin, or on the processivity of the SMC proteins; we thus argue that this synergy may be at work across organisms and throughout the cell cycle.

Genomes are stored in extremely confined and highly crowded environments, yet they must be kept largely free of entanglements during most of the cell cycle. Failing to do so leads to a proliferation of topological issues that can stop gene transcription, DNA replication or cell division, eventually leading to cell death [1–3]. Although TopoII proteins are known to play a crucial role in mediating topological changes on DNA *in vivo* [4], the precise pathways employed by these proteins to maintain the genome disentangled is still poorly understood [1].

In vitro and under dilute conditions, TopoII proteins efficiently resolve topological entanglements and stabilise a population of knotted DNA below the expected value in thermodynamic equilibrium [5]. These findings can be partially explained by a model where TopoII enzymes recognise specific DNA-DNA juxtapositions [6–8]. Yet, how this model can lead to efficient unknotting and unlinking in crowded environments and crumpled DNA or chromatin substrates is unclear [9, 10]. Even more intriguing is the *in vitro* experimental finding that, in presence of polycations [11] or with super-stochiometric abundance of TopoII [12], the action of these proteins may *increase* the topological complexity of the substrates [11, 13, 14].

While it has been suggested that DNA supercoiling may provide a solution for this problem by promoting hooked DNA juxtapositions [15–17], this argument is valid only for naked, highly supercoiled DNAs such as the ones found in bacteria. The understanding of how efficient topological simplification is achieved in eukaryotes where the genome is packaged into chromatin [18] remains, on the other hand, an outstanding and unresolved problem [19].

Here we propose a novel mechanism of efficient topological simplification in DNA and chromatin *in vivo* that is based on the synergistic action of SMC-driven loop extrusion [20–23] (or ratcheted diffusion [24]) and TopoII. Irrespectively of the precise processive mechanism employed by SMC proteins we show that their loading and sliding along chromatin is sufficient to localise any knotted and linked regions in turn catalysing their topological simplification. Our results reveal that this mechanism is independent of either, the degree of condensation of the substrate or environmental crowding, and is therefore likely to lead to unknotting and unlinking even under the extreme packaging conditions of DNA in the cell nucleus. We finally discuss our model in the context of recent experiments showing that SMC proteins are required to achieve correct sister chromatid decatenation in metaphase [25], reporting frequent DNA damage in front of cohesin motion [26] and identifying a remarkable low frequency of knots in intracellular chromatin [19].

Results and Discussion

Model and System Set Up

We perform Brownian Dynamics (BD) simulations of a generic polymer substrate modelled as a semi-flexbile bead-spring circular chain of 500 beads of size σ, taken to be 2.5 nm for DNA [5] and 10 or 30 nm for chromatin [27]. This model captures physical properties expected for generic polymeric substrates [28] and we consider knotted and linked chains as representative of topological entanglements typically occurring in genetic materials [2, 9, 29, 30] (see Fig. 1). Note that we focus on circular chains to simplify the computational task of monitoring the topological changes of the substrate but, as we discuss below, this is not a crucial requirement for the proposed mechanism to work.

Unlike previous works [28, 31], we employ a model of chromosomes that forbids strand-crossing events. This is achieved by imposing that any pair of consecutive beads along the chain are connected by finitely extensible (FENE) springs [32] while non-consecutive ones are subject to a purely repulsive (WCA) potential. By adding a Kratky-Porod term with a given bending modulus we describe chains with $l_p = 20\sigma$. Note, however, that the results are not qualitatively affected by this choice.

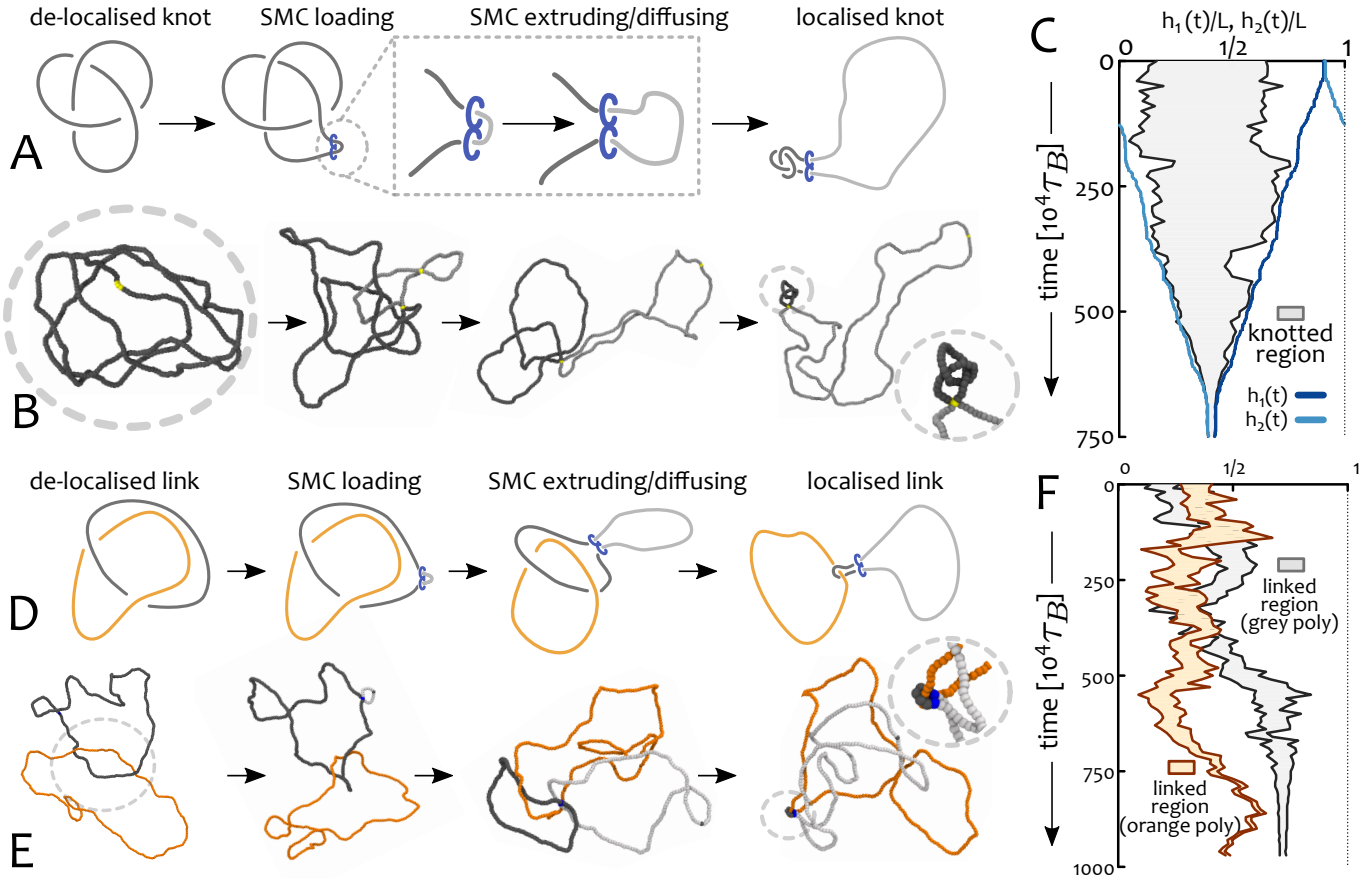

Figure 1: **Sliding of SMC proteins Localises Topological Entanglements.** (A) Schematics of knot localisation starting from a fully delocalised trefoil via loop extrusion. (B) Corresponding Brownian Dynamics simulations. (C) Kymograph showing the shortest knotted arc along the chain as a function of time. The blue curves show the position of the SMC heads $(h_1(t), h_2(t))$ and demonstrate that the knot localises over time. (D) Schematics of link localisation starting from a delocalised Hopf link. (E) Corresponding Brownian Dynamics simulations. (F) Kymograph showing the shortest linked segments for the two polymers. As the SMC protein is loaded on the grey polymer, the linked region in the sister strand is free to slide and this gives rise to a localised but fluctuating orange-shaded area in the figure (SMC heads are not shown for clarity). See Supplementary Movies 1 and 2.

A slip-link model for SMC

The SMC family of proteins, including condensin and cohesin complexes, is a ubiquitous architectural element that plays vital roles in both interphase and mitosis [33], and across organisms [34]. SMC proteins are known to regulate genome architecture by topologically embracing the chromatin fibre [20, 23] and sliding, either processively [35] or diffusively [24, 36], along it.

Based on this evidence, previous works have crudely modelled SMC proteins as harmonic bonds joining two non-consecutive and dynamically updated chromosome segments [21, 22, 31, 37]. In contrast with these models, here we account for both the steric hindrance and the slip-link nature of the SMC complex by forcing the maximum extension of the bond with a FENE potential so that it is energetically unfavorable for a third bead to cross through the gap in between the joined segments.

The two chromosome segments bound by the SMC protein at time t (or the SMC "heads") are denoted as $h_1(t)$ and $h_2(t)$ and updated at rate κ (see SI). Since we focus on processive complexes, the location of the heads is updated as $h_1(t+dt) = h_1(t) + 1$ and $h_2(t+dt) = h_2(t) - 1$, if the Euclidean distance between the next pair of beads is shorter than 1.3σ, or kept still otherwise. This rule ensures that no third bead can pass through the segments bonded by the SMC protein during the update step and it effectively slows down the processivity of the complex depending on DNA structure. Yet, we stress that the speed of the extrusion (or diffusion) process does not qualitatively affect the synergistic mechanism found here, only its overall completion time.

Loop Extrusion or Ratcheted Diffusion of SMC Proteins Localises Topological Entanglements

Thermally equilibrated knotted or linked polymers in a good solvent display topological entanglements that are naturally only weakly localised [38–40]: this means that the "size" of the entanglement [41] grows sublinearly with the length of the whole molecule (see Fig. 1A) [40–42]. Finite size effects and large persistence lengths generally enhance the spreading of the entanglement [38] and this trend is dramatically en-

hanced under confinement [43, 44] and for polymers within crowded environments [45], all conditions typically found *in vivo*. The spreading of entanglements likely hinders TopoII-mediated simplification of the substrate and it is thus natural to ask if there exists a physiological mechanism that may counteract this topological de-localisation *in vivo*.

To address this question we performed BD simulations initialised from equilibrated conditions displaying de-localised entanglements and, at time $t = 0$, we loaded a SMC complex at a random position along the substrate (Fig. 1A). The ensuing extrusion, or growth, of the subtended loop can be monitored by tracking the location of the SMC heads $h_1(t)$ and $h_2(t)$ (see blue curves in Fig. 1C). At the same time, we used well-established existing algorithms [42, 43] (publicly accessible through the server `http://kymoknot.sissa.it` [46]) to compute the knot size – i.e., the shortest portion of the chain hosting the knot. [Note that this is a "physical knot" as a closure procedure is required before its identification through topological invariants.] We observed that the knot (grey shaded area in Fig. 1C), initially spanning a large portion of the polymer, progressively shrinks into a region whose boundaries match the location of the SMC heads. Notably, in the large time limit, all the essential crossings forming the knot (in this case a trefoil, 3_1) were observed to be localised within a segment much shorter than the full polymer length (see Fig. 1B). A similar localisation effect could be achieved on a pair of Hopf-linked polymers (2_1^2, see Fig. 1D-F).

It is important to stress that the discovered SMC-mediated localisation effect is not strictly due to the processivity of the protein and may also be achieved even if SMC slides diffusively along DNA [24]. To localise an entanglement via diffusing slip-link-like elements one would require a number of SMC proteins that increases with the entropic pressure of the knot (or link) which needs to be overcome [47]. Additionally, we highlight that a mechanism of ratcheted diffusion with specific loading sites for the SMC protein (such as NIPBL for the SMC cohesin complex [48]) would further enhance the efficiency of topological localisation with respect to diffusive SMC loaded randomly along the fibre [24].

We conclude this section by mentioning that this localisation mechanism does not require a circular substrate to function. Indeed, physiologically occurring loops – for instance between enhancer and promoters [18], CTCF [49] or those mediated by protein bridges [50] – define transient genomic regions that can be effectively be thought of as looped. We envisage that the SMC-localisation mechanism would thus localise entanglements that become transiently trapped within these looped regions.

A model for SMC-recruited TopoII

Having shown that SMC complexes can induce the *localisation* of topological entanglements, we next asked whether SMC-mediated recruitment of TopoII could provide a fast and efficient mechanism for topological *simplification*.

To this end, and in contrast with previous works which approximated the action of TopoII via a uniform non-zero probability of strand-crossing events over the whole polymer contour [31, 52, 53], here we assume that TopoII is locally recruited by the SMC complex and that it is placed on the outside of the loop subtended by the complex [26, 51]. Thus, only the two nearest beads in front of the ones forming the SMC heads, i.e. $h_{1/2}(t) \pm 1$, $h_{1/2}(t) \pm 2$, were bound by TopoII and allowed to undergo strand-crossing events (see Fig. 2A,B). To this end, we set their interaction with all other beads to be a soft repulsion $U_{\text{Topo}} = A\,[1 + \cos(\pi r/r_c)]$, where the energy barrier A was set to $20k_BT$ for the bead closest to SMC and to $5k_BT$ for the next-nearest bead (this was done to avoid numerical instabilities due to abrupt changes in the force field).

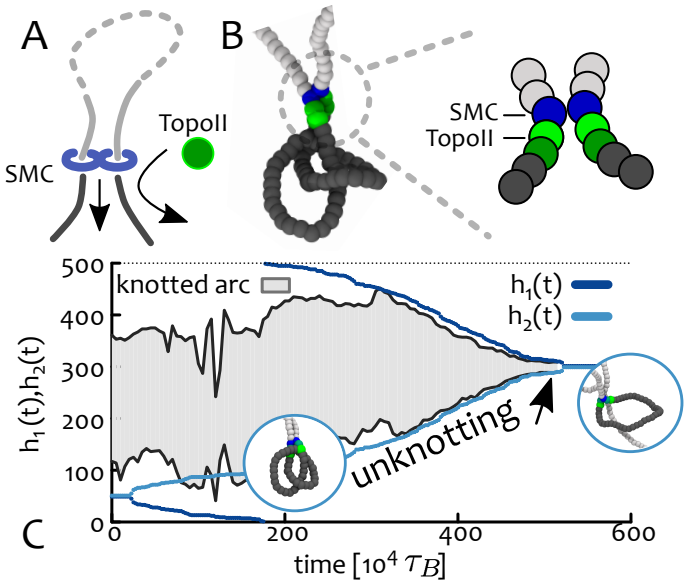

Figure 2: (A) Modelling direct recruitment of TopoII by SMC proteins. As suggested by experimental findings [51], TopoII displays co-localisation with SMC and it is specifically found on the outside of the SMC-mediated loop [26] (dark segments). (B) Implementation of (A) in a bead-spring polymer model: the SMC slip-link is enforced by a FENE bond between blue beads which are updated in time while TopoII action is modelled via soft repulsion of selected (green) beads with all other others bead, thus leading to possible strand crossing, see text). Dark and light green beads have different energy barriers against overlapping ($5k_BT$ and $20k_BT$, respectively). (C) Kymograph showing synergistic knot simplification by SMC and TopoII: SMC-driven loop-extrusion localises the knotted segment (in this case a trefoil 3_1, see snapshot) while TopoII eliminates the crossings. To determine the location and bounds of the knot we employed the algorithm described in Refs. [42, 43, 46]. A running average over 5 timesteps was employed to ease visualisation. See Suppl. Movie 3.

Localisation of Topological Entanglements Catalyses TopoII-mediated Simplification

To see whether a synergistic mechanism coupling SMC extrusion to TopoII-mediated strand crossing could systematically simplify the substrate topology, we performed BD simulations initialised from equilibrated configurations containing a de-localised trefoil knot (3_1) and loaded one SMC pro-

tein recruiting a TopoII enzyme, as discussed in the previous section (see Fig. 2). We monitored the time evolution of the substrate topology by computing its instantaneous Alexander polynomial [46] while tracking both the position of the SMC heads and the boundaries of the knotted region [42]. Remarkably, in all the independent replicas of the system, the SMC-TopoII complex was able to simplify the topology of the substrate down to the unknot.

Importantly, we observed that the topological simplification occurred only after the localisation of the knotted region by the SMC protein (see Fig. 2C). This can be explained by the argument that a localised knot breaks the symmetry between the region inside it and outside it along the polymer, so that intra-chain contacts are more likely to occur between segments forming the local knot than between any other two segments of the polymer. In turn, this localisation favours the undoing of essential crossings. In other words, knot (or link) localisation increases the local entropic pressure within a knotted region [47] which then promotes the knot (or link) simplification.

We stress that the observed systematic topological simplification is different from all existing alternative mechanisms accounting for the action of TopoII alone [52, 54]. Our mechanism also works in the absence of high levels of supercoiling, which is known to provide another avenue to post-replicative decatenation [17] – this is important as highly supercoiled conformations are not documented for eukaryotic chromatin.

	Synergistic		RP (Free)		HJ (Free)
	Free	Confined	Ref. [52]	Ref. [57]	Ref. [55]
$7_2 \to K$	0	0.02	–	0.5	–
$7_2 \to 5_2$	0.31	0.43	–	0.25	–
$7_2 \to 5_1$	0	0.02	–	0.005	–
$7_2 \to 0_1$	0.69	0.52	–	0.24	–
$7_1 \to K$	0.02	0.06	–	0.66	–
$7_1 \to 5_1$	0.98	0.92	–	0.34	–
$7_1 \to 3_1$	0	0.02	–	0	–
$6_1 \to K$	0	0.04	0.15	0.3	–
$6_1 \to 4_1$	0.39	0.33	0.53	0.44	–
$6_1 \to 0_1$	0.61	0.63	0.32	0.26	–
$5_2 \to K$	0	0.1	0.11	0.49	0.26
$5_2 \to 4_1$	0.02	0	0	0	0
$5_2 \to 3_1$	0.5	0.25	0.53	0.2	0.23
$5_2 \to 0_1$	0.48	0.65	0.36	0.31	0.51
$5_1 \to K$	0	0.06	0.15	0.69	–
$5_1 \to 3_1$	1	0.94	0.85	0.31	–
$4_1 \to K$	0	0.04	0.08	0.16	–
$4_1 \to 0_1$	1	0.96	0.92	0.84	–
$3_1 \to K$	0	0.15	0.1	0.22	0.2
$3_1 \to 0_1$	1	0.85	0.9	0.78	0.8

Table I: Comparison between transition probabilities arising from synergistic simplification mechanism (this work), in free and confined ($\langle R_g \rangle / R_c \simeq 3$) cases, versus RP and HJ models in unconfined conditions. Here, $k_1 \to K$ denotes transitions to a knot K with minimal crossing number (MCN) larger than or equal to that of the starting knot k_1. (HJ, hooked juxtaposition; RP, Random Passage).

Synergistic Topological Simplification is Efficient also in Crowded and Confined Conditions

One of the major problems in elucidating how TopoII-mediated topological simplification works *in vivo* is that it must somehow be able to "recognise" the global topology of the underlying DNA molecule while performing local strand-crossings. Hooked DNA juxtapositions between pre-bent segments may provide a simple read-out mechanism to simplify localised knots in dilute conditions [6, 52, 55]. However, this is not a viable pathway in crowded or confined conditions such as those *in vivo* for at least two reasons: (i) in dense solutions many DNA-DNA juxtapositions will occur by random collision regardless of the local bending and (ii) knots and other forms of topological entanglement tend to de-localise under (isotropic) confinement [43]. In this context we asked whether the synergistic mechanism proposed here may instead provide a robust pathway to carry out simplifications of genomic topologies under confinement, as required within the nucleus of cells.

To answer this question we performed simulations where several knots, ranging from the trefoil (3_1) to the 9_1, were confined within a sphere of radius R_c, smaller than the typical size of the same polymer in equilibrium with a good solvent, $\langle R_g \rangle$. Under confinement, knots are strongly delocalised [43] (see Fig. 3), yet we discover that the synergistic action of SMC and TopoII can still efficiently simplify the substrate topology until it becomes eventually unknotted. As the SMC protein slides along the crumpled substrate, we observe configurations in which a third segment is found in front of the extruding fork can spontaneously occur (see Fig. 3). These conformations are reminiscent of hooked juxtapositions [54, 55] that are here due to the linear reeling of the substrate through the SMC slip-link. These findings also suggest that the recruitment of TopoII in front of the extruding motion of the SMC [51], may have been evolved as an optimal strategy to resolve topological entanglements which may cause DNA damage if unresolved.

We highlight that a mechanism that can achieve topology simplification under confinement has never been proposed before. In marked contrast with existing models, our simulations even suggest that SMC-driven simplification may be more efficient under stronger confinement (see SI). This can be explained as the entropic penalty for forming a loop of size l by the SMC complex is smaller on a crumpled substrate than on an unconfined, and thus swollen, one [24]. For this reason, the extruding action of the SMC complex is less hindered under confinement and the localisation of the knot is achieved more quickly (see SI, Fig. S2).

Whilst the action of a single SMC always led to the localisation of both a knot and its essential crossing, this was no longer the case when we accounted for the simultaneous (and parallel) action of multiple SMC. Indeed, we observed that the extrusion of non-nested loops may stabilise a de-localised knot whose essential crossings are localised (see SI). This mixed state is akin to that recently observed during the translocation of knotted DNA through nanopores [56] and will be further investigated in the future.

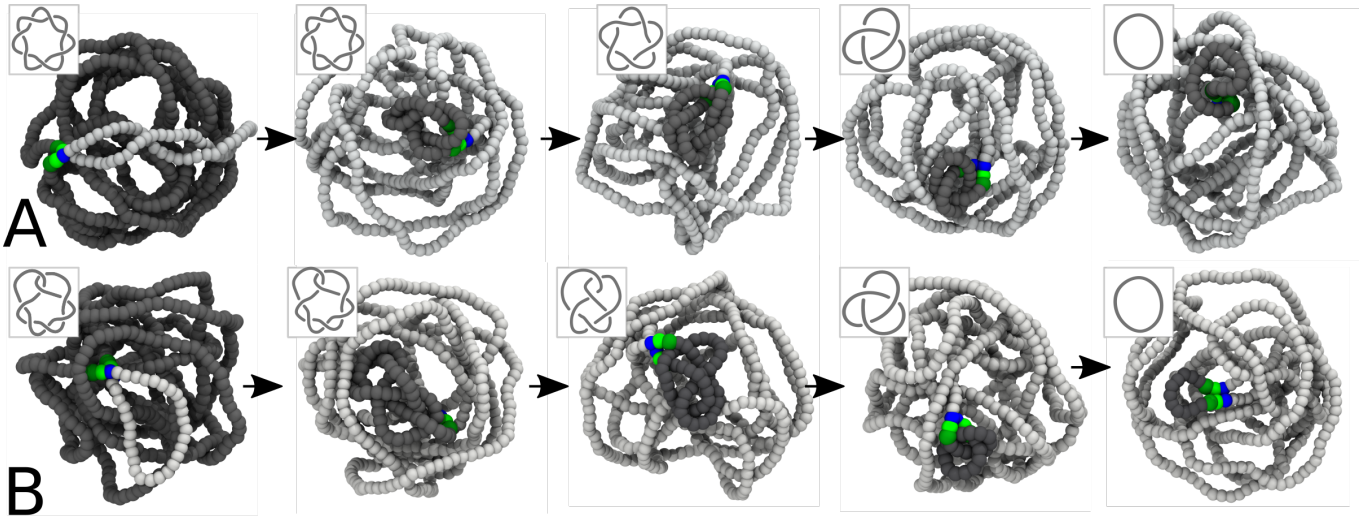

Figure 3: **Efficient Unknotting under Confinement.** The synergistic action of SMC and TopoII proteins can systematically simplify knotted substrates even under confinement. Here we show the case of a torus (7_1) and a twist (7_2) knots confined within a sphere with radius R_c, such that $\langle R_g \rangle / R_c \simeq 3$. In the snapshots, light-grey beads are the ones that have been extruded by, hence behind, the SMC. Dark-grey beads are the ones outside the extruded loop. Blue beads mark the location of the SMC heads. Green and dark-green beads mark the location of TopoII, as described in the text. (A) Unknotting of a 7_1 knot through the "cascade" of torus knots 5_1 and 3_1. (B) Unknotting of a 7_2 knot through 5_2 and 3_1 knots. Direct simplification $7_2 \rightarrow 0_1$ is also observed in more than half of the simulations (see Table TI), this is because twist knots have unknotting number 1. See Suppl. Movies 4 and 5.

Comparison of the Synergistic Versus Random Passage and Hooked Juxtaposition Models

To compare the efficiency of the synergistic simplification mechanism proposed here with previous models of TopoII-mediated action, we estimated the transition probabilities within the space of knots [52], $\rho(\mathcal{K}_1 \rightarrow \mathcal{K}_2)$ by performing 50 simulations starting from equilibrated polymers tied in the form of knots ranging from 3_1 to 7_2. The transition probabilities are reported in Table TI, both for unconstrained and confined polymers, and are compared with those reported by random passage [52, 57] (RP) and hooked juxtaposition [55] (HJ) models.

Whereas in RP and HJ models the transition probabilities are computed from a set of equilibrium polymer conformations, our transition probabilities are non-equilibrium ones. Indeed, our model has an absorbing state which is attained when the SMC has extruded the full polymer and simplified its topology down to the unknot. In this state, because the remaining polymer segments are no longer able to cross each-other, the topology is locked in the trivial one at all future times. The values reported in table TI for $\rho(\mathcal{K}_1 \rightarrow \mathcal{K}_2)$ should thus be understood as the (asymmetric) probability that, starting from a polymer with given topology $\mathcal{K}_1$, the next topology attained by the polymer is $\mathcal{K}_2$. In this sense, our transition rates can be compared with the ones reported for the RP and HJ models. Unlike these and other models, ours predicts a virtually systematic simplification cascade down to the unknot in both free and confined conditions, such as are found in the cell nucleus.

Conclusions

In this work, we have provided numerical evidence for a new molecular mechanism that can efficiently maintain the genomes free of entanglements. This is based on the combined action of SMC-driven extrusion and TopoII-mediated strand-crossing. More specifically we found that the sliding of molecular hand-cuffs along knotted or linked substrates naturally generates highly localised entanglements which catalyse their simplification through the action of TopoII. Importantly, the envisaged mechanism is universal, in that it works equally well on DNA or chromatin, open or circular substrates, interphase and mitosis (in eukaryotes) and across all life forms that have evolved TopoII-like and SMC-like proteins.

Our findings provide a mechanistic explanation for existing evidence suggesting that the presence of both SMC condensin and TopoII, is required to ensure correct decatenation of sister chromatids [58–60] and that inactivation of SMC leads to an increase in entanglement complexity and sister chromatids intertwining [25]. In our model, SMC-driven knot and link localisation is indeed an essential step to avoid the creation of more complicated knots and links which may occur under the extreme packing typically achieved in mitosis.

It is also interesting to highlight that recent experiments reported that in absence of TopoII, DNA damage is accumulated in front of cohesin complexes [26]. This finding is in agreement with the principle revealed by our model, i.e. that the sliding motion of SMC entraps topological entanglements and, in turn, accumulates local stress promoting DNA breaks. In this respect, we argue that our results provide compelling mechanistic evidence that there is an evolutionary advantage for TopoII proteins to be actively recruited by SMC complexes since this process contributes to release the accumulated stress during the dynamic formation of looped domains [26].

An analogous mechanism to that uncovered here may work to efficiently eliminate entanglements during DNA replication. Here, two replication forks moving along opposite directions along the genome (or reeling it in) effectively extrude a DNA or chromatin loop [61]. The polymerising machinery at the fork then effectively functions as a SMC, driving the localisation of entanglements ahead of the growing loop. As TopoII is known to act in front of the replication fork [62], the very same synergistic mechanism for topological simplification proposed here may be at play in this context as well. It is also of interest to note that PCNA, the molecular clamp associated with a processive polymerase [63], also recruits components of repair complexes, which would again be evolutionary advantageous to resolve entanglement-related DNA damage. All these considerations reinforce the idea that the mechanism we propose may be universal.

Whilst we assumed for simplicity that SMC moves unidirectionally, due to either an intrinsic motor activity or a motor pushing it from behind, we expect that similar physics should be at work for diffusively sliding SMC complexes, provided that entropic considerations favour loop enlargement. This will be the case if SMC is loaded at particular sites, as this creates a positively biasing osmotic pressure [24], or when multiple slip-links are simultaneously present, as the entropy is generically maximised when some of the loops shrink to zero [47].

We finally speculate that the remarkable low knotting probability recently quantified in intracellular chromatin and its weak or absent scaling with the length of the substrate [19] may be explained by the model proposed in this work: indeed, the SMC-TopoII synergistic topological simplification is remarkably insensitive to substrate length (see SI) since TopoII is always recruited to act on a localised knot or entanglement.

We hope that, based on the evidence reported here, new experimental effort will identify and further characterise this novel synergistic mechanism to regulate genome topology. For instance, we envisage that it may be tested *in vivo* by combining the action of TopoII and functional SMC [35, 36] and *in vivo* by quantifying chromatin knotting [19] after knockdown of SMC rather than TopoII.

Acknowledgements This work was supported by the ERC CoG 648050 THREEDCELLPHYSICS.

[1] A. Bates and A. Maxwell *DNA topology* Oxford University Press (2005)
[2] J. M. Sogo et al. *J. Mol. Biol.* **286**(3), 637 (1999)
[3] G. Jannink et al. *Biophys. J.* **71**(July), 451 (1996)
[4] J. C. Wang *Quarterly reviews of biophysics* **31**(2), 107 (1998)
[5] V. V. Rybenkov et al. *Proc. Natl. Acad. Sci. USA* **90**(11), 5307 (1993)
[6] A. V. Vologodskii et al. *Proc. Natl. Acad. Sci. USA* **98**(6), 3045 (2001)
[7] J. Yan et al. *Nature* **401**(October), 932 (1999)
[8] Z. Liu et al. *J. Mol. Biol.* **400**(5), 963 (2010)
[9] J. Arsuaga et al. *Proc. Natl. Acad. Sci. USA* **99**(8), 5373 (2002)
[10] B. Martínez-García et al. *Nucleic Acids Res.* **42**(3), 1821 (2014)
[11] M. Krasnow and N. Cozzarelli *J. Biol. Chem* **257**, 2687 (1982)
[12] S. A. Wasserman and N. R. Cozzarelli *J. Biol. Chem.* **266**(30), 20567 (1991)
[13] T. Hsieh and D. Brutlag *Cell* **21**, 115 (1980)
[14] T. Hsieh *J Biol CheM* **258**(20), 8413 (1983)
[15] A. Vologodskii and N. R. Cozzarelli *Biophys J.* **70**(6), 2548 (1996)
[16] G. Witz et al. *Proc. Natl. Acad. Sci. U. S. A.* **108**(9), 3608 (2011)
[17] D. Racko et al. *Nucleic Acids Res.* (July), gkv683 (2015)
[18] B. Alberts et al. *Molecular Biology of the Cell* Taylor & Francis (2014)
[19] A. Valdés et al. *Nucleic Acids Res.* **46**(2), 650 (2018)
[20] K. Nasmyth *Annu Rev Gen* **35**(1), 673 (2001)
[21] E. Alipour and J. F. Marko *Nucleic Acids Res.* **40**(22), 11202 (2012)
[22] G. Fudenberg et al. *Cell Rep.* **15**(9), 2038 (2016)
[23] F. Uhlmann *Nat. Rev. Mol. Cell. Biol.* **17**(April) (2016)
[24] C. Brackley et al. *Phys. Rev. Lett.* **119**(13), 138101 (2017)
[25] E. Piskadlo et al. *Elife* **6**, 1 (2017)
[26] L. Vian et al. *Cell* **173**, 1 (2018)
[27] J. Dekker et al. *Science* **295**(5558), 1306 (2002)
[28] A. Rosa and R. Everaers *PLoS Comp. Biol.* **4**(8), 1 (2008)
[29] S. Trigueros and J. Roca *BMC Biotechnol.* **7**(1), 94 (2007)
[30] D. Marenduzzo et al. *Proc. Natl. Acad. Sci. USA* **106**(52), 22269 (2009)
[31] A. Goloborodko et al. *Compaction and segregation of sister chromatids via active loop extrusion* Technical report (2016)
[32] K. Kremer and G. S. Grest *J. Chem. Phys.* **92**(8), 5057 (1990)
[33] T. Hirano *Cell* **164**(5), 847 (2016)
[34] T. B. Le et al. *Science* **342 VN -**(6159), 731 (2013)
[35] A. M. Ganji et al. *Science* **7831**(February), 1 (2018)
[36] M. Kanke et al. *EMBO J.* pages 1–13 (2016)
[37] A. L. Sanborn et al. *Proc. Natl. Acad. Sci.* **112**(47), 201518552 (2015)
[38] E. Orlandini et al. *Phys. Biol.* **6**(2), 025012 (2009)
[39] A. Y. Grosberg and Y. Rabin *Phys. Rev. Lett.* **99**(21), 1 (2007)
[40] M. Caraglio et al. *Scientific Reports* (2017)
[41] B. Marcone et al. *Journal of Physics A: Mathematical and General* **38**(1), L15 (2005)
[42] L. Tubiana et al. *Prog. Theor. Phys. Suppl.* **191**(191), 192 (2011)
[43] L. Tubiana et al. *Phys. Rev. Lett.* **107**(18), 1 (2011)
[44] D. Marenduzzo et al. *Proc. Natl. Acad. Sci. USA* **110**(50), 20081 (2013)
[45] G. D'Adamo and C. Micheletti *Macromolecules* **48**(17), 6337 (2015)
[46] L. Tubiana et al. *EPJ E* **41**(6), 72 (2018)
[47] R. Zandi et al. *arxiv:0306587* (2003)
[48] J. Zuin et al. *Proc. Natl. Acad. Sci. USA* **111**(3), 996 (2014)
[49] S. S. P. Rao et al. *Cell* **159**(7), 1665 (2014)
[50] C. A. Brackley et al. *Proc. Natl. Acad. Sci. USA* **110**(38), E3605 (2013)
[51] L. Uusküla-Reimand et al. *Genome Biol* **17**(1), 1 (2016)
[52] A. Flammini et al. *Biophys. J.* **87**(5), 2968 (2004)
[53] D. Michieletto et al. *Phys. Biol.* **12**(1), 036001 (2015)
[54] A. V. Vologodskii *Nucleic Acids Res.* **37**(10), 3125 (2009)
[55] Y. Burnier et al. *Nucleic Acids Res.* **35**(15), 5223 (2007)
[56] A. Suma and C. Micheletti *Proc. Natl. Acad. Sci. USA* pages

E2991–E2997 (2017)
[57] X. Hua et al. *Topology and its Applications* **154**(7), 1381 (2007) special Issue: The Third Joint Meeting Japan-Mexico in Topology and its Applications
[58] J. Baxter and L. Aragón *Trends Genet.* **28**(3), 110 (2012)
[59] N. Sen et al. *Mol. Cell* **64**(1), 134 (2016)
[60] E. Piskadlo and R. A. Oliveira *Int. J. Mol. Sci.* **18**(12), 1 (2017)
[61] P. R. Cook *Science* **284**(5421), 1790 (1999)
[62] J. Roca *Nucleic Acids Res.* **37**(3), 721 (2008)
[63] T. S. Krishna et al. *Cell* **79**(7), 1233 (1994)
[64] A. Goloborodko et al. *bioRxiv* page 021642 (2015)
[65] D. Michieletto et al. *Phys. Rev. X* **6**, 041047 (2016)
[66] C. R. Calladine et al. *Understanding DNA: the molecule and how it works* volume 1 Elsevier Academic Press (1997)
[67] J. H. Gibcus et al. *Science* **359**(6376) (2018)
[68] D. Michieletto *Soft Matter* **12**, 9485 (2016)
[69] M. Baum et al. *Nat. Commun.* **5**, 4494 (2014)
[70] S. Plimpton *J. Comp. Phys.* **117**(1), 1 (1995)
[71] P. G. D. Gennes *Scaling concepts in polymer physics* (1979)
[72] A. Vologodskii *Phys. Life Rev.* **18**, 118 (2016)

Supplementary Information

Appendix A: Computational Details

A Polymer Model for Chromatin and DNA substrates

We model a polymer substrate, such as DNA or chromatin, as a chain of beads of size σ connected by springs. This types of models are widely employed in the literature and have been shown to faithfully capture the physical behaviour of DNA and chromatin [28, 37, 64, 65]. To ensure that the polymer substrates does not cross through itself, we impose that any two beads (a, b) at distance r are subject to a purely repulsive (WCA) potential

$$U^{ab}_{WCA}(r) = k_B T \left[4 \left[\left(\frac{\sigma}{r}\right)^{12} - \left(\frac{\sigma}{r}\right)^{6} \right] + 1 \right] \text{ if } r \leq 2^{1/6}\sigma \tag{A1}$$

and 0 otherwise. Further, we impose that consecutive beads are connected by finitely extensible (FENE) springs modelled as

$$U^{ab}_{FENE}(r) = -\frac{k_f R_0^2}{2} \ln \left[1 - \left(\frac{r}{R_0}\right)^2 \right] \text{ if } r \leq R_0 \tag{A2}$$

and ∞ otherwise. Here, $k_f = 30\epsilon/\sigma^2$ and $R_0 = 1.5\sigma$ are typical parameters employed to prevent spontaneous chain crossing [32]. We account for DNA or chromatin stiffness by adding a potential controlling the angle formed by consecutive triplets of beads

$$U^{ab}_{KP} = \frac{k_B T l_p}{\sigma} \left[1 - \frac{\boldsymbol{t}_a \cdot \boldsymbol{t}_b}{|\boldsymbol{t}_a||\boldsymbol{t}_b|} \right], \tag{A3}$$

where $\boldsymbol{t}_a$ and $\boldsymbol{t}_b$ are the tangent vectors connecting bead a to $a+1$ and b to $b+1$ respectively; l_p is the persistent length of the chain and by setting $l_p = 20\sigma = 50$ nm we model an average DNA sequence [66] while with $k_\theta = 3\,k_B T$ we account for a more flexible polymer with $l_p = 3\sigma = 90$ nm such as a 30nm chromatin fibre [27].

A Model for Structural Maintenance of Chromosome Proteins

The SMC proteins – such as cohesins and condensins – are a well-known and widely studied family of proteins [33] that have now been identified as responsible for dynamic genomic loops in both inter- and meta-phase [26, 67]. These proteins can be crudely viewed as physical slip-links [68] that embrace one, or two, double-stranded DNA and slide along DNA/chromatin [23, 24] in turn stabilising the formation of dynamic loops [22, 24] and halting at "anchor" points embodied by converging CTCF proteins [26, 49]. In this work, we aim to mechanistically investigate the generic effect of SMC proteins on topological entanglements – such as knots and links – that may be present on DNA or chromatin in interphase and mitosis. To this end, we propose a generic model where SMC proteins loaded on the polymer are described as bonds connecting two non-consecutive beads along the chain. Importantly, and in marked contrast with recent models of loop extrusion [22, 31, 37], here we account for the physical presence of a slip-link-like molecule joining two segments of chromosomes by forcing the maximum extension of the bond with a FENE potential so that it is energetically very unfavourable for a third bead to cross through the gap in between the joined segments. Again, this is done to prevent spontaneous events that would change the local topology of the substrate and that are not physically possible in real situations. It is worth noting that this detail has not been correctly accounted for in some of the existing models of loop extrusion [22, 37]. In other words, the SMC protein is modelled by including a potential

$$U^{h_1 h_2}_{SMC}(r) = -\frac{k_f R_0^2}{2} \ln \left[1 - \left(\frac{r(h_1, h_2)}{R_0}\right)^2 \right] \text{ if } r \leq R_0 \tag{A4}$$

where h_1 and h_2 are the instantaneous position of the two segments of chromosome bound by the SMC protein at time t (or the SMC "heads"). At rate $\kappa = 10^{-3}\tau_B^{-1}$ ($\tau_B \equiv \sigma^2/D$ is the Brownian time of a bead, see below), we change the position of the heads via the following protocol:

$$\begin{cases} h_1(t+dt) = h_1(t) + 1 \text{ and} \\ h_2(t+dt) = h_2(t) - 1 \text{ if } d(h_1, h_2) \leq 1.3\sigma \\ h_1(t+dt) = h_1(t) \text{ and} \\ h_2(t+dt) = h_2(t) \text{ otherwise or if } h_1 = h_2\,. \end{cases} \tag{A5}$$

In other words, the SMC enlarges the loop formed by two monomers on average every 1000 Brownian times only if the distance between the next pair of beads is shorter than 1.3σ in 3D space. This choice ensures that no third bead can pass through the beads bonded by the SMC protein and it effectively slows down the processivity of the complex from $v = 2\sigma\kappa = 2\ 10^{-3}\sigma/\tau_B$ to about $v \simeq 5\,10^{-5}\sigma/\tau_B$. Yet, we stress that the speed of the extrusion (or diffusion) process does not affect the efficiency of the synergistic mechanism we uncover in this work.

Mapping to Real Units

Given the size of a bead σ and the energy scale k_BT (at room temperature), we can derive the typical (Brownian) time taken for a bead to diffuse its own size as $\tau_B = \sigma^2/D = 3\pi\eta\sigma^3/k_BT$. Using the viscosity of the nucleoplasm $\eta \simeq 200cP$ [69] we obtain that our simulated Brownain time corresponds to $\tau_B = 7\mu$s for DNA and $\tau_B = 12$ ms for a 30nm chromatin fibre. The initial state of our simulations is an equilibrated polymer conformation (without SMC proteins acting on it) that is obtained running 10^5 τ_B steps, i.e. of the order of seconds for DNA and tens of minutes for chromatin. Production runs in which SMC proteins are loaded on the polymer also typically cover 10^5 τ_B steps which we find is enough for complete knot localisation.

Topoisomerase Model

In contrast to previous works which crudely model the action of TopoII as a uniform non-zero probability of strand-crossing events [28, 31, 53], here we assume that TopoII is locally recruited by the SMC protein and it is loaded on the outside of the loop subtended by the complex. Thus, here only the two beads (about 60 nm) in front of the ones forming the SMC complex – i.e. if $h_{1,2}(t)$ are the positions of the SMC heads then $(h_1(t)+1,\, h_1(t)+2)$ and $(h_2(t)-1,\, h_2(t)-2)$ are the beads associated to TopoII – are allowed to undergo strand-crossing events. In other words, we set their interaction with all other beads as a soft repulsion

$$U_{Topo} = A\left[1+\cos\left(\frac{\pi r}{r_c}\right)\right]. \tag{A6}$$

To avoid numerical instabilities which may occur due to the dynamic update of the SMC heads, we tune A so that it displays an increasing energy gradient, i.e. the furthest bead from the SMC complex is set to have $A = 5k_BT$ while the closer one $A = 20k_BT$. This ensures that when the position of the SMC is updated no two beads interacting through the WCA potential are (even partially) overlapping.

Integration Procedure

The total energy field experienced by bead a is the sum of all the pairwise and triplet interactions involving all other beads, i.e.

$$U_a = \sum_{b\neq a}\left[U^{ab}_{WCA} + \left(U^{ab}_{FENE} + U^{ab}_{bend}\right)\left(\delta_{b,a+1}+\delta_{b,a-1}\right)\right] + \\ + U^{ab}_{SMC}(t)\delta_{a,h_1}\delta_{b,h_2}\,, \tag{A7}$$

where the Kronecker deltas $\delta_{i,j}$ indicate that bond and angle potentials are restricted to consecutive beads along the polymer and that the SMC potential is acting on the beads corresponding to the SMC heads. The time evolution of each bead in the system is thus governed by the following Langevin equation,

$$m_a\frac{d^2\vec{r}_a}{dt^2} = -\nabla U_a - \gamma_a\frac{d\vec{r}_a}{dt} + \sqrt{2k_BT\gamma_a}\vec{\eta}_a(t), \tag{A8}$$

where m_a and γ_a are the mass and the friction coefficient of bead a, and $\vec{\eta}_a$ is its stochastic noise vector obeying the following statistical averages:

$$\langle\boldsymbol{\eta}(t)\rangle = 0; \quad \langle\eta_{a,\alpha}(t)\eta_{b,\beta}(t')\rangle = \delta_{ab}\delta_{\alpha\beta}\delta(t-t'), \tag{A9}$$

where the Latin indices represent particle indices and the Greek indices represent Cartesian components. The last term of Eq. (A8) represents the random collisions caused by the solvent particles and, for simplicity, we assume all beads have the same mass and friction coefficient (i.e. $m_a = m$ and $\gamma_a = \gamma$) and finally set $m = \gamma = k_B = T = 1$. Equation (A8) is integrated using a standard velocity-Verlet algorithm, which is performed using the Large-scale Atomic/Molecular Massively Parallel Simulator (LAMMPS) [70]. For the simulation to be efficient yet numerically stable, we set the integration time step to be $\Delta t = 0.01\,\tau_B$, where τ_B is the Brownian time as mentioned previously.

Appendix B: Localisation Efficiency as a function of Number of SMC

It is reasonable to ask whether the synergistic effect we uncover in this work may be made more efficient by considering multiple SMC extruding loops on the same substrate. To answer this question we perform simulations in which we simultaneously load 1, 2 and 4 SMC complexes at a random position along a polymer which is tied in a trefoil knot. The interaction between SMC heads is here considered mutually exclusive, i.e. if two SMC heads are found on consecutive beads and moving in opposite directions they remain still as cannot overlap on the same bead. In these simulations we discover two seemingly counter-intuitive effects:

1. the knots which become localised do so in shorter time when multiple SMC are loaded (Fig.S S1A);
2. the probability to find a localised knot (here practically defined as one made by less than 50 beads) at large times decreases with the number of SMC (Fig.S S1B);

The former finding can be readily explained by the fact that multiple SMC can extrude more contour length on the same unit of time. Yet, the decrease in localisation probability is more puzzling.

By close inspection of the simulation trajectories we discover that this reduction in localisation probability is due to situations in which two or more SMC proteins are simultaneously loaded within and outside a knotted region. These situations may lead to trapped conformations that stabilise a delocalised knotted state (see kymograph and snapshots Fig. S1). On the contrary, a single SMC, even if loaded within a knotted region can turn the knot "inside-out" and ultimately generate a fully localised knot.

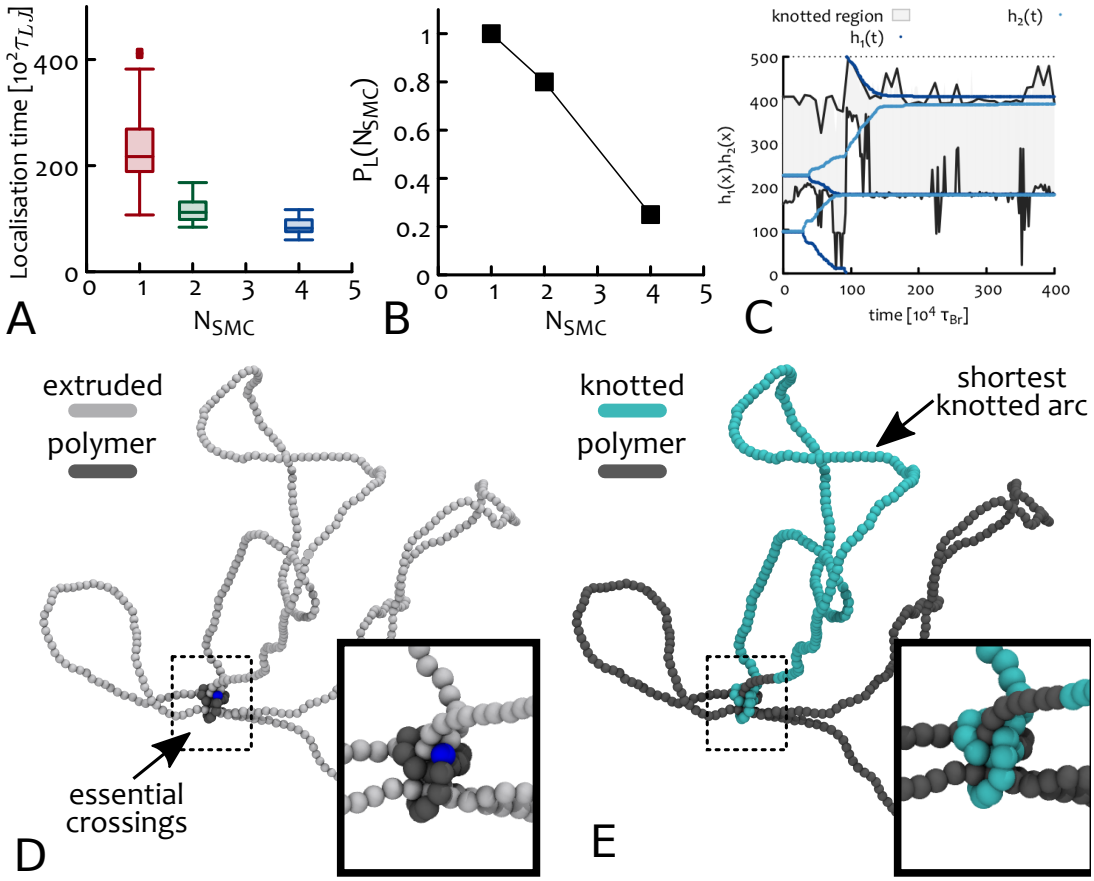

Figure S1: (A) Box plots showing the distribution of localisation times on a polymer substrate $N = 500$ beads long and with SMC moving at rate $\kappa = \tau_{Br}^{-1}$. [Here a knot is considered localised if its shortest arc spans less than 50 beads]. (B) Probability to find a localised knot at large times as a function of the number of SMC proteins simultaneously loaded on the substrate. (C) Kymograph of a simulation for a polymer tied in a trefoil knot and with 2 SMC loaded at time $t = 0$. The shortest arc that can be defined knotted (after suitable closure [43]) is shaded in grey. The 4 SMC heads are shown in shades of blue. One of the two SMC is loaded within the knotted region at time $t = 0$, whereas the other is outside it. Eventually, heads belonging to different SMC meet and stall, thereby stabilising a delocalised knot. (D) Snapshot from the same simulation used to generate (C) and showing extruded segments in light grey and the polymer backbone in dark grey. One can see that essential crossings are localised (inset). (E) Snapshot highlighting the shortest arc that can be defined knotted in blue, while the rest of the polymer is showed in dark grey. These snapshots shows that even if essential crossings are localised, the knot itself need not be. This conformation has been recently found in simulations of translocation of knotted DNA [56]). See Supplementary Movie M6.

Appendix C: Synergistic Unknotting is Favoured Under Confinement

As mentioned in the main text, we find that the proposed synergistic mechanism between SMC and TopoII can simplify knots even under strong confinement. Because of this, we argue that this pathway may be at work in vivo. Here, we further characterise this finding by quantifying the rate of knot localisation as a function of confinement. To this end, we perform different sets of 40 independent simulations in which a trefoil knot tied along a $N = 300$ beads polymer is confined within a sphere of varying radius R_c and subject to the action of a single SMC. We consider a range of values for R_c ranging from tight confinement $R_c = 10\sigma \simeq \langle R_g \rangle/3$ to $R_c = 50\sigma > \langle R_g \rangle$, where $\langle R_g \rangle$ is the typical size of the polymer in equilibrium in good solvent and under no confinement.

Remarkably, we discover that the typical localisation time (here practically defined as the first time at which the shortest knotted arc spans less than 50 beads) is shorter the stronger is the confinement (see Fig. S2). We argue that this puzzling finding can be explained by the following argument: the entropic penalty associated with the formation of a loop of length l is $S/k_B \sim c \log l$ where c is the exponent determining the decay of the contact probability $P_c(l) \sim l^{-c}$. For a crumpled polymer, i.e. the conformation assumed under confinement, the contact exponent $c = \nu d = 1$, whereas for a swollen coil in good solvent (self-avoiding), $c \simeq 2.1$ [71]. For this reason, the entropic penalty grows more steeply for a swollen coil than for a crumpled globule. In turn, this implies that the loop extruding action of the SMC protein is entropically favoured (or less hindered) under confinement, in qualitative agreement with our findings (see Fig. S2).

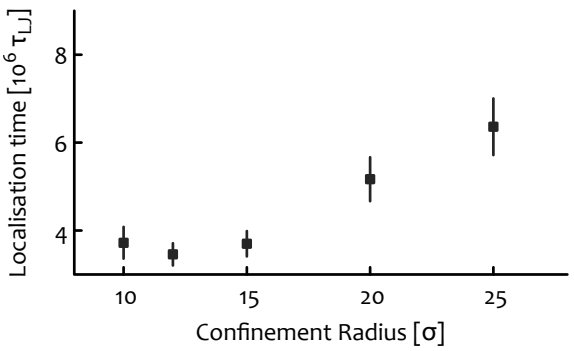

Figure S2: Average localisation time of a trefoil knot tied along a polymer $N = 300$ beads long, under confinement within a sphere and subject to the action of a single SMC moving at rate $\kappa = 0.1\tau_{Br}^{-1}$. The error bars represent the standard error of the mean.

	$M = 300$	$M = 500$	$M = 1000$	$M = 2000$
$7_1 \to K$	0	0.02	0	0.1
$7_1 \to 5_1$	1	0.98	1	0.9
$5_1 \to K$	0	0	0	0.03
$5_1 \to 3_1$	1	1	0.97	0.97
$5_1 \to 0_1$	0	0	0.03	0
$3_1 \to K$	0	0.02	0	0.03
$3_1 \to 0_1$	1	0.98	1	0.97

Table S1: Comparison of unknotting pathways for a 7_1 knot tied along a polymer of length M in unconfined conditions and subject to the synergistic unknotting. To obtain this table, 50 independent simulations were initialised from a 7_1 state and the transition to other knot types recorded. $k_1 \to K$ denotes a transition to any knot type with minimal crossing number larger than k_1.

Appendix D: Synergistic Unknotting as a Function of Substrate Length

In this section we provide a more quantitative, albeit not definitive, examination of efficiency of the proposed synergistic simplification as a function of the length of the substrate. Because of the largely fluctuating 3D conformations assumed by long polymers, the random passage and hooked juxtaposition models are known to be sensitive on this parameter [72]. To compare these models with the one proposed here, we perform 4 sets of 50 independent simulations starting from an equilibrated (and unconfined) polymer tied as a 7_1 knot with varying length M, ranging from 300 to 2000. If one takes $\sigma = 2.5$ nm as the diameter of DNA, then this range compares to $750 - 5000$ bp. In Table T S1 we report the values of the transitions $k_1 \to k_2$ observed for these different lengths of the substrate.

As one can notice, we find that for $M = 300$ the 7_1 is taken to the unknot through 5_1 and 3_1 with probability 1 and this probability is only mildly, if at all, affected for longer substrates. We highlight that this finding is likely to due to the fact that TopoII strand-crossing occurs more likely in pre-localised topological entanglements, thus strongly biasing their simplification over their complication.

In other words, while the time to localise a knot increases on longer substrates, the simplification cascade towards the unknot is virtually unaffected. In light of this insensitivity, we reason that if this mechanism was at work in vivo, then the knot probability in intracellular chromatin should not depend on the length of the fibre under consideration (because the efficiency to remove entanglements is the same no matter its length). Intriguingly, this picture is in remarkable agreement with recent experimental findings [19].